Asian Journal of Chemistry; Vol. 25, No. 15 (2013), 8455-8459

ASIAN JOURNAL OF CHEMISTRY

http://dx.doi.org/10.14233/ajchem.2013.14784

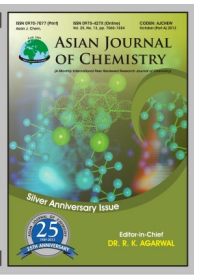

Absorption Properties of Co-Ce Codoped $TiO_2/SiO_2/NiFe_2O_4$ Mesoporous Microspheres

ZHAOHUI OUYANG[1,2,*], LIN WU[1] and DELIAN YI[1]

[1]College of Chemical Engineering and Technology, Wuhan University of Science and Technology, Wuhan 430081, P.R. China
[2]Wu Han Qing Jiang Chemical Industry Company Limited, Wuhan 430081, P.R. China

*Corresponding author: E-mail: ouyang_3h@163.com

(*Received*: 5 November 2012; *Accepted*: 24 August 2013) AJC-13972

By using nanoparticles $NiFe_2O_4$ as magnetic carrier, the polystyrene-$SiO_2/NiFe_2O_4$ magnetic microspheres were prepared from styrene, tetraethoxysilane, by emulsion polymerization using 3-methacryloxypropyltrimethoxysilane as a cross-linking agent. (Co,Ce)-$TiO_2/SiO_2/NiFe_2O_4$ multilayer magnetic mesoporous microspheres material were prepared by sol-gel process with tetrabutyl titanat as raw materials Co, Ce as codoped agent, PS-$SiO_2/NiFe_2O_4$ particle as the core, sodium dodecyl sulphate and polyvinylpyrrolidone as templating agent. The complex permittivity and permeability of composites made from (Co, Ce)-$TiO_2/SiO_2/NiFe_2O_4$ multilayer magnetic mesoporous microspheres material embedded in paraffin matrix separately are measured by voter network analyzer and the reflectivity is calculated within 1-18 GH. The absorption mechanisms of magnetic mesoporous microspheres material are studied based on the electromagnetic wave propagation laws in lossy medium. The microwave absorption properties of the multilayer composite film are excellent. The maximum microwave loss efficiency reaches 31 dB and the continuous frequency range with the loss above 20d B reaches 2 GHz.

Key Words: Absorption, Co-Ce, Codoped, $TiO_2/SiO_2/NiFe_2O_4$.

INTRODUCTION

It is well known that ideal absorbing materials have the characteristics of strong absorption, broad-band, thin thickness and light quality. So far, however, it is not found that the materials can completely meet these requirements and therefore appropriate modification and design of existing materials become the focus in research[1,2]. The ferrite is a double-complex medium, it not only has a general medium characteristics of ohmic loss, polarization loss, ion and electron resonance loss, but also has strong domain wall resonance loss, magnetic moments natural resonance loss and particle resonant loss. It has excellent microwave properties and acts as the main material in the microwave absorption technique[3,4]. Since it is difficult for single ferrite absorbing materials to meet the requirements of broad absorption band, high absorption rate and thin thickness, it is required to add some additives to make composite ferrite absorbers with better matched electromagnetic parameters[5]. Co, Ce co-doped magnetic mesoporous composite microspheres were prepared using $NiFe_2O_4$ nanoparticles as magnetic phase, Co and Ce as doping ions, silica, titanium dioxide as a non-magnetic phase to improve the effective absorption of electromagnetic energy in broad-band.

EXPERIMENTAL

Styrene (AR Analytical reagent) was used after vacuum distillation. Polyvinyl pyrrolidone, ammonium persulphate, sodium bicarbonate, sodium dodecyl sulphate, polyoxyethylene octylphenol ether, iron nitrate nonahydrate, nickel nitrate, cobalt(II) nitrate hexahydrate, cerium(III) nitrate, urea, ethanol, *n*-butyl titanate, ethyl silicate and 3-methacryloxypropyltrimethoxysilane were commercially available products and used without further purification.

Preparation of $NiFe_2O_4$ nanoparticles: Molar ratio of $Fe(NO_3)_3{\cdot}9H_2O$, $Ni(NO_3)_2{\cdot}6H_2O$ and $CO(NH_2)_2$ was dissolved in a certain amount of deionized water and mixed evenly. The resulting mixture was transferred to the autoclave and heated at 180-200 ºC for 4 h. $NiFe_2O_4$ particles were obtained after cooling naturally, solid-liquid separation, washing and drying.

Preparation of polystyrene-$SiO_2/NiFe_2O_4$: $NiFe_2O_4$ particles were added to ethanol solution. After ultrasound and stirring for 0.5 h, TEOS/ ethanol was added to the solution and $NH_3{\cdot}H_2O$ was added dropwise to adjust pH value. $SiO_2/NiFe_2O_4$ microspheres were obtained after filter, washing and drying.

Deionized water, a small amount of anionic emulsifier sodium dodecyl sulphate and non-ionic emulsifier polyoxyethylene octylphenol ether, were added to a four-necked flask

with reflux condenser and nitrogen protection. The emulsion solution was heated to 60 ºC in water bath. 3-Methacryloxypropyltrimethoxysilane and $SiO_2/NiFe_2O_4$ microspheres were added to styrene monomer and then treated with ultrasound for 10 min. The mixture solution was added to the emulsion system with initiator ammonium persulphate and buffer $NaHCO_3$. The emulsion solution was heated to 80 ºC for 1.5 h and then 90 ºC for 0.5 h. Polystyrene/$SiO_2/NiFe_2O_4$ microspheres were obtained after demulsification, washing and drying.

Preparation of (Co,Ce)-$TiO_2/SiO_2/NiFe_2O_4$: Sodium dodecyl sulphate and polyvinyl pyrrolidine were added to a four-necked flask with deionized water and the solution was adjusted by hydrochloric acid to pH value of 2. A mixed solution of tetrabutyl titanate and ethanol was added dropwise to the four-necked flask and then anhydrous ethanol solution of cobalt nitrate and cerium nitrate pentahydrate was rapidly added to the flask. After stirring for 1 h, the resulting polystyrene/$SiO_2/NiFe_2O_4$ microspheres were added to the mixture solution using ammonia to adjust the pH value. The (Co,Ce)-TiO_2/PS/$SiO_2/NiFe_2O_4$ microspheres were obtained after washing and drying.

Characterization: The crystal structure and surface morphology of Co-Ce Codoped $TiO_2/SiO_2/NiFe_2O_4$ magnetic mesoporous microspheres were characterized by X-ray diffraction (XRD) S-4800 high-resolution field emission scanning electron microscope. The wave-absorbing capacity of the sample was performed on an Agilent 8720 vector network analyzer using coaxial ring specimens with the inner diameter of 3 mm, the outside diameter of 7 mm and the height of 2-4 mm.

RESULTS AND DISCUSSION

Morphology and diameter of (Co,Ce)-$TiO_2/SiO_2/NiFe_2O_4$: The scanning electron microscopy (SEM) image (Fig. 1) reveals the morphology of (Co,Ce)-TiO_2/polystyrene/$SiO_2/NiFe_2O_4$ microspheres calcined directly with diameter of 30-50 nm. Compared with polystyrene/$SiO_2/NiFe_2O_4$ microspheres, the diameter of (Co,Ce)-TiO_2/PS/$SiO_2/NiFe_2O_4$ is significantly increased. Polymer magnetic microspheres are burned and decomposed at high temperatures to produce large amounts of gas, which results in discontinuity and pore collapse of the face. (Co,Ce)-TiO_2/PS/$SiO_2/NiFe_2O_4$ microspheres are dissolved in DMF and then calcined at 500 ºC to remove residual organic matter to obtain (Co,Ce)-$TiO_2/SiO_2/NiFe_2O_4$ microspheres. As shown in Fig. 2, the diameter of round granular microspheres changes little, surface pore size remains uniform and no collapse appears.

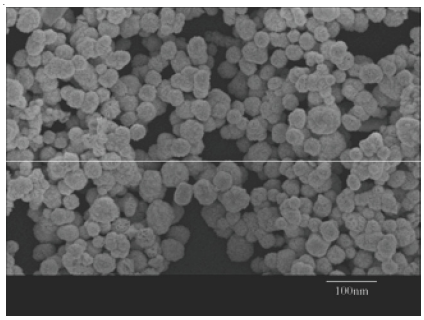

Fig. 1. SEM image of (Co,Ce)-$TiO_2/SiO_2/NiFe_2O_4$ calcined directly

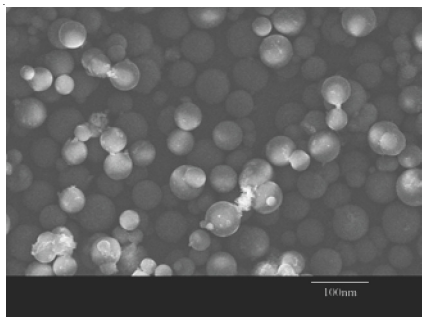

Fig. 2. SEM image of (Co,Ce)-$TiO_2/SiO_2/NiFe_2O_4$ dissolved and calcined

Crystal structure of the composite: The crystal structure of the composite was characterized by a Bruker M18XHF diffractometer and the X-ray diffraction pattern of the composites is presented in Fig. 3.

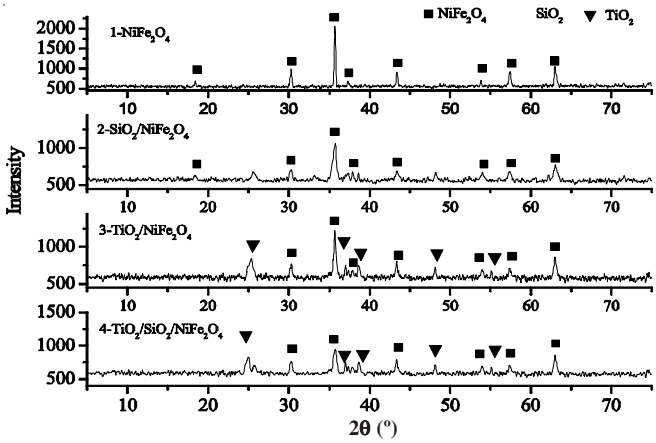

Fig. 3. XRD graph of magnetic powders

The X-ray diffraction pattern of $NiFe_2O_4$ is shown in spectrum 1 of Fig. 3. No impurities such as NiO, FeO, $Ni(OH)_2$, $Fe(OH)_3$ can be found from the pattern. The $NiFe_2O_4$ samples exhibit a face-centered cubic spinel structure. As shown in spectrum 2, a very small peak at 250 shows that the silica coated on $NiFe_2O_4$ surface is an amorphous structure without complete silica grains. No peaks of rutile-type titanium dioxide can be found from the spectra 3 and 4 and the peaks could be indexed as the anatase type. No peaks of CoO and CeO can be observed in the spectrum 4.

Complex permittivity of composite microsphere: The molar ratio of Ce: Co: TiO_2 in composite microsphere is 0.05:0.08:1 and the quality rate of SiO_2: $NiFe_2O_4$ is 0.1. The influence of the titanium dioxide on the electromagnetic parameters of composites is investigated and the real and imaginary part of the complex permittivity and magnetic permeability are shown in Figs. 4-7, respectively. The composite dielectric constant changes obviously after adding with non-metallic phase. The uniform SiO_2 insulating film isolates the nickel ferrite particles in composite microspheres, which reduces the polarization of the particles as the electric dipole and leads to lower its intrinsic dielectric constant ε_m. Meanwhile, the insulating film blocks the conductive network formed by the magnetic powder and reduces the conductivity of the entire network[6]. According to the formula of $\varepsilon'' = \sigma/\omega$, network conductivity decreases with the decrease of the imaginary

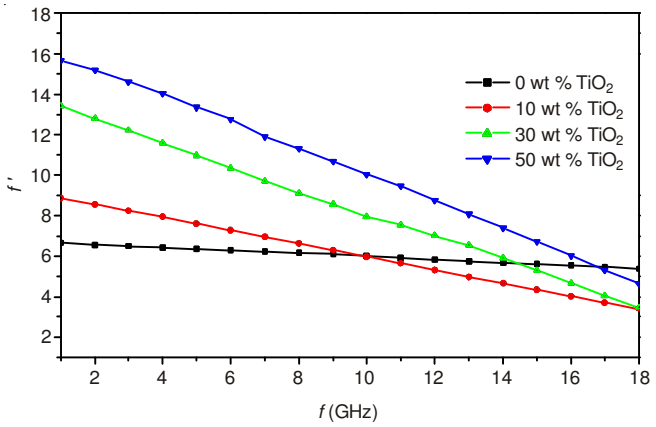

Fig. 4. Real permittivity of magnetic powders as a function of frequency

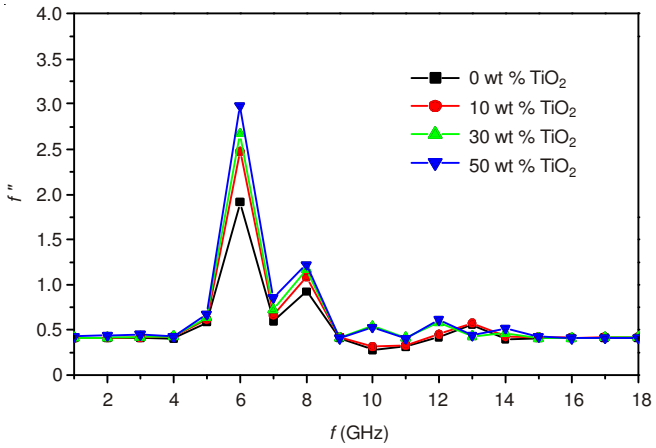

Fig. 5. Imaginary permittivity of magnetic powders as a function of frequency

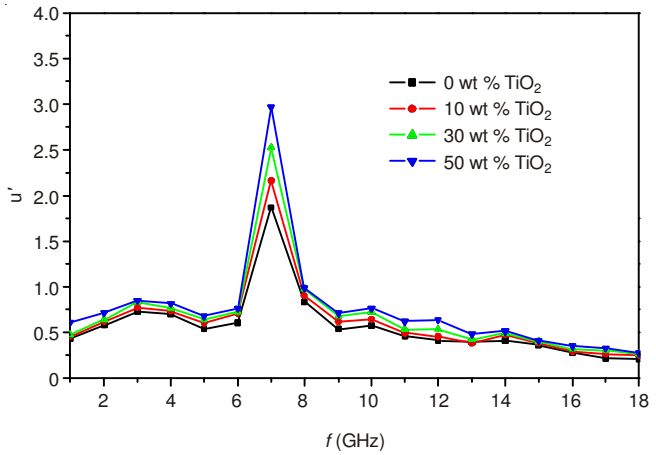

Fig. 6. Real permeability of magnetic powders as a function of frequency

part of dielectric constant[7,8]. In addition, the mesoporous surface of the composite microspheres and Co, Ce doped inorganic ion generate two-phase interface, which can introduce the appropriate amount of air and help to reduce the dielectric constant of the composite microspheres. As can be seen from the dielectric loss factor, in the low-frequency, it changes greatly due to interfacial polarization produced by the interface air. Since composite microspheres are blended with titanium dioxide, the surface of microspheres contains a lot of oxygen vacancy defects after sintering at N_2 atmosphere. The impurity levels in the band gap of these defects will be excited and

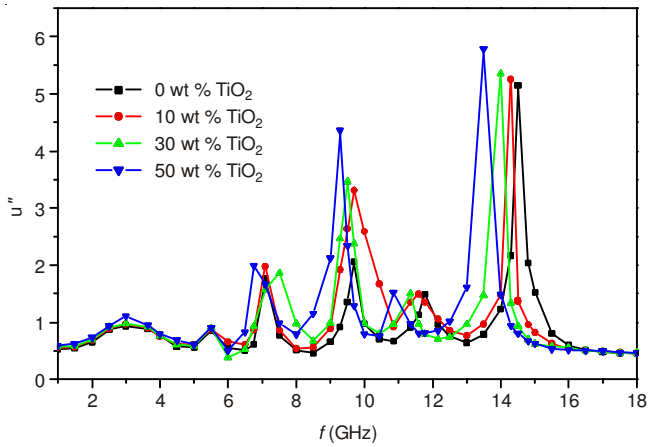

Fig. 7. Imaginary permeability of magnetic powders as a function of frequency

generated free carriers to make the increase of surface photovoltaic effect higher than the decrease of that due to the presence of the impurity level. With the role of the external electric field, the carriers excited by the forbidden band defect levels generate the space charge redistribution on the surface to form space charge polarization and significantly improve the dielectric properties[9]. The imaginary part of the complex permittivity of the composite materials is significantly greater than that of the ferrite, so that the dielectric loss of the ferrite is improved.

As shown in Fig. 4, the titanium dioxide content of the non-magnetic phase increases in the low frequency region and the real part of the complex permittivity of the composite microspheres increases. With the increase of test frequency, the real part of the complex permittivity of the composite is gradually decreased. The real part of the complex dielectric constant of the composite is smaller than pure nickel ferrite in the high-frequency band. It can be seen that the addition of titanium dioxide and silica has an impact on the ability of energy storage, which is increased in the low frequencies and decreased with the increase of frequencies. In Fig. 5, the imaginary part ε" of complex dielectric constant is changed with adding of the non-magnetic phase. The peak in frequency spectrum of the dielectric loss appears in low frequencies and the result shows that the relaxation polarization phenomena exhibit inside the materials with the role of the external electric field.

Relative complex permeability of magnetic powders: The effect of non-magnetic phase on the complex magnetic permeability is weak. A peak in the spectrum of the complex magnetic permeability appears in the frequency slightly higher than the 7 GHz. The materials can absorb and store a certain amount of magnetic energy. As the frequency is gradually increased, the real part of the complex magnetic permeability of the composites and the nickel ferrite gradually decreases. After combination with non-magnetic phase, the imaginary part of the complex permeability of the nickel ferrite is shown in Fig. 7 and the result shows that the imaginary part of the complex magnetic permeability of the composites has a significant change.

The absorption peak of the materials represents the absorption of external electromagnetic energy in the imaginary part

spectrum of the complex permeability and the iron magnetic resonance is the main absorption mechanism. The frequency position of ferromagnetic resonance is dependent on the size of the anisotropy field of the composites. The anisotropy field is derived from the interaction of lattice anisotropy constant and the saturation magnetization. Titanium dioxide added in the composites has an impact on the internal lattice structure of the ferrite, thus changing the anisotropy constant of the ferrite. TiO_2 has obvious improvement on the complex magnetic permeability, but increases the real part and the imaginary part of the dielectric constant to a larger extent[10]. The introduction of Ce can significantly improve the electromagnetic properties of the ferrite and markedly increased the imaginary part and the real part of the magnetic permeability[11]. Co d-electron shell admits seven electrons, including three single-electrons with electronic spin magnetic moment of 3 μB. They are magnetic metal ions, which can improve the magnetic properties of the composite microspheres. SiO_2 as a low dielectric material has the limited impact on the magnetic permeability, the modification of SiO_2 and the doping of Co and Ce can effectively inhibit the increase of the real and imaginary part of the complex permittivity.

Impedance and the amplitude attenuation of the intrinsic magnetic mesoporous particles: According to electromagnetic wave theory, the propagation coefficient of the electromagnetic wave within the medium $K = j\frac{2\pi f}{c}\sqrt{\varepsilon\mu} = j\frac{2\pi f}{c}\sqrt{(\varepsilon' - j\varepsilon'')(\mu' - j\mu'')} = \alpha + \beta$, where α and β are the attenuation coefficient and the phase constant, respectively[12]. Absorbing materials with excellent microwave absorbing properties are required not only to have a strong electromagnetic attenuation capacity, but also to make the electromagnetic waves enter the materials. The former can be characterized by the attenuation coefficient α and the latter is dependent on the intrinsic impedance η, both can be expressed as:

$$\alpha = \frac{\sqrt{2}\pi f}{c}[\sqrt{(\varepsilon''\mu'' - \varepsilon'\mu')^2 + (\varepsilon'\mu'' + \varepsilon''\mu')^2} + (\varepsilon''\mu'' - \varepsilon'\mu')]^{1/2} \quad (1)$$

$$\eta = \sqrt{\frac{\mu}{\varepsilon}} = R + jX \quad (2)$$

The intrinsic impedance and the amplitude attenuation coefficient e-2dα can be calculated on combining the formulas (1) and formula (2) and the results are shown in Figs. 8 and 9. They decide jointly the location and size of the microwave loss.

Magnetic mesoporous particles microwave loss: The microwave electromagnetic parameters of Figs. 4-7 are is substituted into the reflectance formula of the monolayer absorbing materials[13].

$$RL = 20\log\left|\frac{Z_{in} - Z_0}{Z_{in} + Z_0}\right| \quad (3)$$

$$Z_{in} = \sqrt{\frac{\mu_0\mu}{\varepsilon_0\varepsilon}}\tanh\left(j\frac{2\pi fd}{c}\sqrt{\varepsilon\mu}\right) \quad (4)$$

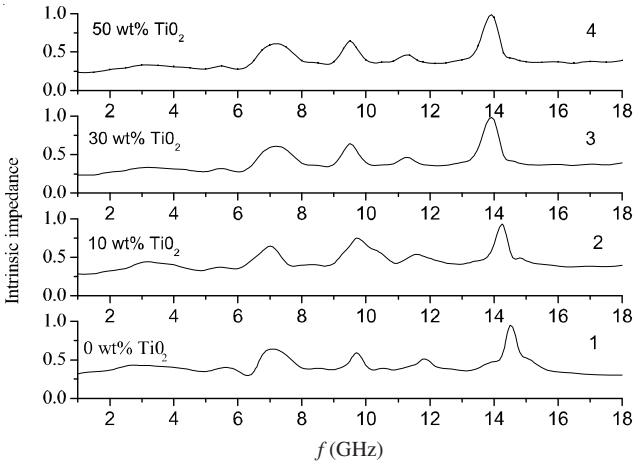

Fig. 8. Intrinsic impedances of magnetic powders as a function of frequency

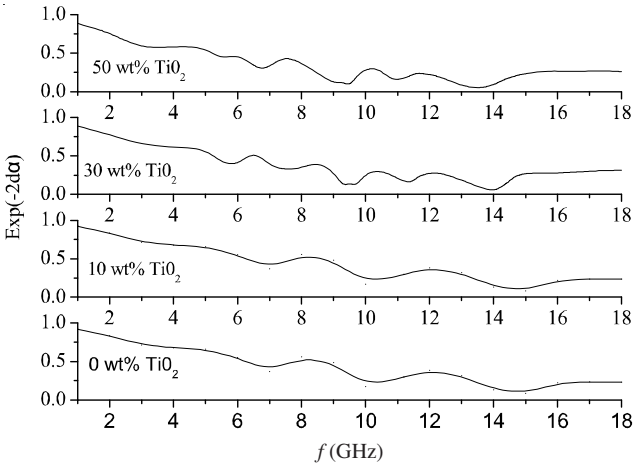

Fig. 9. Attenuation coefficients of magnetic powders as a function of frequency

$$Z_0 = \sqrt{\frac{\mu_0}{\varepsilon_0}} \quad (5)$$

where RL is the reflectance, Z is the input impedance, Z_0 is the air resistance, f is the frequency and d is the coating thickness, c is the speed of light and μ_0 and ε_0 are the vacuum magnetic permeability and dielectric constant, respectively. The results are shown in Fig. 10.

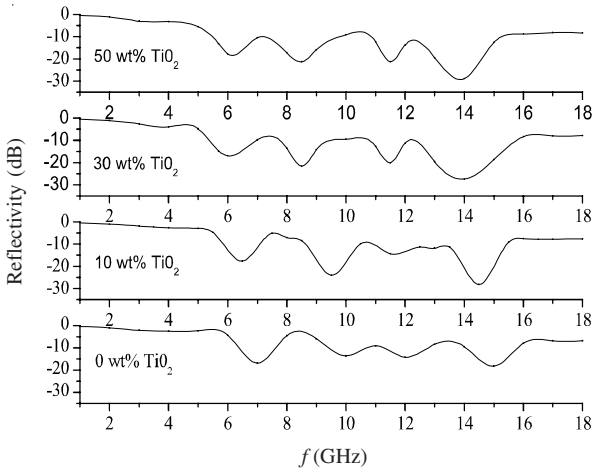

Fig. 10. Calculated reflectivity curves of single absorber as a function of frequency

As can be seen from Fig. 10, the absorption peak of the absorbing materials shifts to the low frequency and the absorbing bandwidth of the composites are significantly better than that of the nickel ferrite. In addition of 30 % titanium dioxide in composite materials, the maximum loss of the composites reaches 31dB and the width of continuous frequency with the depletion efficiency more than 20dB is close to 2GHz the depletion efficiency is more than 20dB continuous frequency. For ferrite, the magnetic loss is the main channels to absorb the electromagnetic energy. It is the most effective and direct way to increase the values and move frequency position of the imaginary part of the complex magnetic permeability to improve the ferrite microwave loss. In Fig. 7, the imaginary part of the complex permeability has a noticeable change after adding a nonmetallic phase. Loss degree of each sample of microwave energy is different except for the absorption frequencies in the loss spectrum of the microwave energy. The changes of the intrinsic impedance η and amplitude attenuation coefficient the $e^{-2d\alpha}$ of the composites are consistent.

Conclusion

The introduction of non-magnetic substance of titania and silica causes the change of dielectric constant of the composites with the increase of the imaginary part of the complex permeability and the enhancement of the dielectric loss and the magnetic loss. In the composite microspheres, the introduction of Ce and Co, can obviously improve the electromagnetic properties of the ferrite. The coupling between the ferrite and non-magnetic nanoparticles can reduce the anisotropy field of the ferrite and improve microwave absorption properties. The ferrite and non-magnetic composite microspheres were prepared using the sol-gel method. The absorption peak of the samples shifts to the low frequency and the maximum loss of the composites reach 31dB. The width of continuous frequency with the depletion efficiency more than 20dB is close to 2GHz.

ACKNOWLEDGEMENTS

This work was financially supported by Wuhan Qing Jiang Chemical Industry Company Limited. The authors are grateful to Research and Development Center of Wu Han Qing Jiang Chemical Industry Company Limited.

REFERENCES

1. K.S. Lee, Y.C. Yun, I.B. Jeong and S.S. Kim, *Mater. Sci. Forum*, **534-536**, 1465 (2007).
2. Z.M. Dang and L.Z. Fan, *Chem. Phys*., **369**, 95 (2003).
3. T. Giannakopoulou, L. Kompotiatis, A. Kontogeorgakos and G. Kordas, *J. Magnet. Magnet. Mater*., **246**, 360 (2002).
4. M.A. Ahmed, N. Okasha and R.M. Kershi, *Mater. Chem. Phys*., **113**, 196 (2009).
5. J. Wang, H. Zhang, S.X. Bai and K. Chen, *J. Funct. Mater. Devices*, **13**, 318 (2007).
6. Y.Q. Pang, H.F. Cheng and G.P. Tang, *J. Mater. Res*., **23**, 652 (2009).
7. M.Z. Wu, Y.D. Zhang, S. Hui, T.D. Xiao, W.A. Hines, J.I. Budnick, and G.W. Taylor, *Appl. Phys. Lett*., **80**, 4404 (2002).
8. J.L. Xie, B.L. Liang and L.J. Deng, *J. Fuct. Mater*., **39**, 41 (2008).
9. S.P. Ruan, W. Dong and F.Q. Wu, *Chem. J. Chin. Univ*., **25**, 484 (2004).
10. J. Zhuang, Y.H. Chi and J.N. Shi, *J. Chin. Rare Earth Soc*., **20**, 324 (2002).
11. J.X. Qiu and M.Y. Gu, *Appl. Surf. Sci*., **252**, 889 (2005).
12. K.D. Zhou, X.W. Zhang and T.L. Dong, Electromagnetic Field Theory Fundamentals, China Machine Press, edn. 2, p. 250 (2000).
13. K.N. Rozanov, *IEEE Trans on Antennas Propagation*, **48**, 1230 (2000).